A Three-Dimensional and Nonlinear Virtual Test Car

Georg Rill*
Department of Mechanical Engineering, OTH Regensburg, Germany

Summary. Virtual testing procedures have become a standard in vehicle dynamics. The increasing complexity of driver assistance systems demand for more and more virtual tests, which are supposed to produce reliable results even in the limit range. As a consequence, simplified vehicle models, like the classical bicycle model or 4-wheel vehicle models, have to be replaced by a fully three-dimensional and nonlinear vehicle model, which also encompasses the details of the suspension systems. This paper presents a passenger car model, where the chassis, the four knuckles, and the four wheels are described by rigid bodies, the suspension system is modeled by the generic design kinematics, and the TMeasy tire model provides the tire forces and torques in all driving situations.

Keywords: Virtual Test Car (VTC), Design Kinematics, TMeasy, Equations of Motion, Transient Response

Introduction

The multibody approach has become a standard in vehicle dynamics [1]. General multibody software packages, like Adams/Car [2], ReCurDyn [3], or SIMPACK [4] make it possible to assemble vehicle models of different complexities. Commercial products, like CarSim [5], CarMaker [6], or DYNA4 [7] provide ready to use vehicle models, which are real-time capable and may be used in Hardware-in-the-Loop (HIL) test rigs, in driving simulators, or for all kind of virtual driving tests including parameter optimization or autonomous drive. A basic multibody model of a standard passenger car is usually supplemented by a handling tire model, like Pacejka [8] or TMeasy [9], and it is extensible by subsystems for the steering system and the drive train [10]. Sophisticated model approaches combined with an efficient and robust solver provide an excellent runtime performance [11]. Nevertheless, simplified and rather crude three-dimensional vehicle models are still applied in the context of lap-time optimization [12] and autonomous driving [13]. However, this reduces such investigations to the level of basic studies, because the impact of the suspension properties and the road roughness on vehicle dynamics is not taken into account. This paper demonstrates, that a virtual test car (VTC), properly modeled by a three-dimensional and nonlinear multibody system, is able to achieve a much faster-than-real-time performance even on standard personal computers, although it includes the nonlinear suspension kinematics and the wheel/tire dynamics.

The VTC-Model

Model Structure

A virtual test car, valid for typical passenger cars in all driving situations, is represented by a three-dimensional multibody model which consists at least of the chassis, four knuckles, and four wheels, Figure 1. The virtual test car (VTC) is

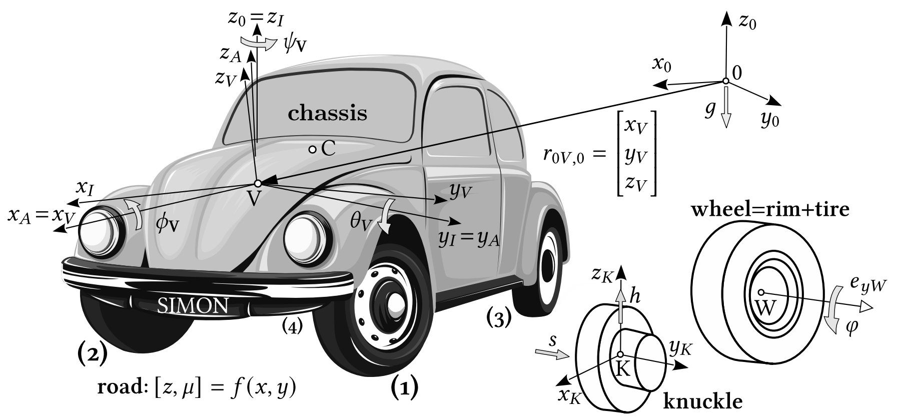

Figure 1: Multibody model structure of a passenger car

operated with the TMeasy tire model, which represents a handling model, where the tire acts as a massless force element. The suspension kinematics allows each knuckle to perform relative to the chassis a hub motion h and a steer motion s. This generic model approach makes it possible to investigate the influence of different suspension designs, including all-wheel steering, on the handling and dynamics of a vehicle. The steer motions of passenger car front wheels are typically coupled by a rack and pinion steering system and the rear suspension often incorporates no active steer motions at all.

Each of the four wheels, consisting of the rim and the tire, rotates with the angle φ about a knuckle-fixed axis, defined by the unit vector e_{yW}. The generalized coordinates x_V, y_V, z_V, ψ_V, θ_V, and ϕ_V describe the momentary position and orientation of the vehicle-fixed, within the VTC model also chassis-fixed, reference frame V with respect to an earth-fixed frame 0. The points C and K denote the gravity centers of the chassis and the knuckle. In practice, the wheels of passenger cars are sufficiently balanced. Then, the wheel center W will be located on the wheel rotation axis and is fixed to the knuckle as a consequence.

The multibody system, providing the basis of three-dimensional passenger car model, has up to $f = 6+4*2+4 = 18$ degrees of freedom if each of the four knuckles is modeled with a hub and a steer motion. The total number of degrees of freedom is reduced to $f = 16$ if the rear wheels are not actively steered. More complex but still real-time capable vehicle models including the drive train, the steering system, and dynamic force elements are described in [11] and [14]. Appropriate road models provide the road height z and the friction coefficient μ as a function of the contact point coordinates x and y [15].

Reference Frame and Nontrivial Generalized Velocities

The momentary position and orientation of the chassis-fixed or vehicle-fixed reference frame V is provided by the position vector $r_{0V,0}$ and the rotation matrix A_{0V} defined in the VTC model as

$$r_{0V,0} = \begin{bmatrix} x_V \\ y_V \\ z_V \end{bmatrix} \quad \text{and} \quad A_{0V} = \begin{bmatrix} \cos\psi_V & -\sin\psi_V & 0 \\ \sin\psi_V & \cos\psi_V & 0 \\ 0 & 0 & 1 \end{bmatrix} \begin{bmatrix} \cos\theta_V & 0 & \sin\theta_V \\ 0. & 1 & 0 \\ -\sin\theta_V & 0 & \cos\theta_V \end{bmatrix} \begin{bmatrix} 1 & 0 & 0 \\ 0 & \cos\phi_V & -\sin\phi_V \\ 0 & \sin\phi_V & \cos\phi_V \end{bmatrix} \tag{1}$$

where x_V, y_V, z_V, ϕ_V, θ_V, and ψ_V serve as generalized coordinates. The comma separated index 0 indicates that the components of the vector r_{0V} pointing from 0 to V are expressed in the earth-fixed reference frame 0.

The components of the velocity vector v_{0V} and the angular velocity vector ω_{0V} can both be expressed in the vehicle-fixed frame. The set of kinematical differential equations

$$\begin{bmatrix} \dot{x}_V \\ \dot{y}_V \\ \dot{z}_V \end{bmatrix} = A_{0V}^T \underbrace{\begin{bmatrix} v_x \\ v_y \\ v_z \end{bmatrix}}_{v_{0V,V}} \quad \text{and} \quad \begin{bmatrix} \dot{\phi}_V \\ \dot{\theta}_V \\ \dot{\psi}_V \end{bmatrix} = \frac{1}{\cos\theta} \begin{bmatrix} \cos\theta & \sin\phi\sin\theta & \cos\phi\sin\theta \\ 0 & \cos\phi\cos\theta & -\sin\phi\cos\theta \\ 0 & \sin\phi & \cos\phi \end{bmatrix} \underbrace{\begin{bmatrix} \omega_x \\ \omega_y \\ \omega_z \end{bmatrix}}_{\omega_{0V,V}} \tag{2}$$

provides then the time derivatives of the generalized coordinates $\dot{x}_V$, $\dot{y}_V$, $\dot{z}_V$, $\dot{\phi}_V$, $\dot{\theta}_V$, $\dot{\psi}_V$ as a function of the generalized velocities v_x, v_y, v_z, and ω_x, ω_y, ω_z. As shown in [16] this particular choice of nontrivial generalized velocities reduces the complexity of the equations of motion significantly.

Relative Kinematics

The vehicle model, shown in Figure 1, consists of $n = 9$ rigid bodies: the chassis, four knuckles, and four wheels. The absolute position and orientation of an arbitrary body j is defined by

$$r_{0j,0} = r_{0V,0} + A_{0V}\, r_{Vj,V} \quad \text{and} \quad A_{0j} = A_{0V}\, A_{Vj} \tag{3}$$

where $r_{0V,0}$ and A_{0V} are defined by (1) and $r_{Vj,V}$ and A_{Vj} describe the position and orientation of body j relative to the vehicle-fixed reference frame V.

The vector of the absolute body velocity v_{0j} can be expressed in the vehicle-fixed frame

$$v_{0j,V} = v_{0V,V} + A_{0V}^T \frac{d}{dt}\left(A_{0V}\, r_{Vj,V}\right) = v_{0V,V} + \omega_{0V,V} \times r_{Vj,V} + \dot{r}_{Vj,V} \tag{4}$$

where according to (2) the components of the vectors $v_{0V,V}$ and $\omega_{0V,V}$ are entirely defined by the nontrivial generalized velocities v_x, v_y, v_z, ω_x, ω_y, ω_z. The movements of body j relative to the vehicle-fixed frame V can be characterized by a certain set of generalized coordinates, which may be collected in the vector y_j. Then, the vector $r_{Vj,V}$ describing the momentary position of body j relative to V depends on this set of generalized coordinates, $r_{Vj,V} = r_{Vj,V}(y_j)$ and its time derivative with respect to frame V results in

$$\dot{r}_{Vj,V} = \frac{d}{dt} r_{Vj,V}(y_j) = \frac{\partial\, r_{Vj,V}}{\partial\, y_j}\, \dot{y}_j = t_{j,V}(y_j)\, \dot{y}_j \tag{5}$$

where the term $t_{j,V}$ represents the partial velocity of the body j motions. Similarly, the vector of the absolute body angular velocity, expressed in the vehicle-fixed frame V, reads as

$$\omega_{0j,V} = \omega_{0V,V} + \omega_{Vj,V} = \omega_{0V,V} + d_{j,V}(y_j)\, \dot{y}_j \tag{6}$$

where the term $d_{j,V}$ describes the partial angular velocity of the body j motions.

The absolute acceleration and the absolute angular acceleration of body j, both expressed in the vehicle-fixed frame V, are at first provided by

$$\begin{aligned} a_{0j,V} &= A_{0V}^T \frac{d}{dt}\left(A_{0V}\, v_{0V,V}\right) = \omega_{0V,V} \times v_{0j,V} \;+\; \dot{v}_{0V,V} + \tilde{r}_{Vj,V}^T\, \dot{\omega}_{0V,V} + \omega_{0V,V} \times \dot{r}_{Vj,V} + \ddot{r}_{Vj,V} \\ \alpha_{0j,V} &= A_{0V}^T \frac{d}{dt}\left(A_{0V}\, \omega_{0V,V}\right) = \omega_{0V,V} \times \omega_{0j,V} \;+\; \dot{\omega}_{0V,V} + \dot{\omega}_{Vj,V} \end{aligned} \tag{7}$$

where the cross product $\dot{\omega}_{0V,V} \times r_{Vj,V}$ was transferred via $\dot{\omega} \times r = -r \times \dot{\omega} = -\tilde{r}\,\dot{\omega} = \tilde{r}^T\dot{\omega}$ to the multiplication of a transposed skew-symmetric matrix with a vector. The velocity $v_{0V,V}$ and the angular velocity $\omega_{0V,V}$ depend entirely on the generalized velocities. The relative velocity $\dot{r}_{Vj,V}$ and the relative angular velocity $\omega_{Vj,V}$ are provided in (5) and (6). Their time derivatives result in

$$\ddot{r}_{Vj,V} = t_{j,V}(y_j)\,\ddot{y}_j + \dot{t}_{j,V}(y_j)\,\dot{y}_j \qquad \text{and} \qquad \dot{\omega}_{Vj,V} = d_{j,V}(y_j)\,\ddot{y}_j + \dot{d}_{j,V}(y_j)\,\dot{y}_j \tag{8}$$

The trivial choice $z_j = \dot{y}_j$ of generalized velocities is always possible. Then (7) reads as

$$\begin{aligned} a_{0j,V} &= \left[\, \mathrm{I}_{3\times3} \;\; \tilde{r}^T_{Vj,V} \;\; \ldots t_{j,V} \ldots \right] \dot{z} \,+\, \omega_{0V,V} \times (v_{0j,V} + \dot{r}_{Vj,V}) + \dot{t}_{j,V}\dot{y}_j \;=\; \frac{\partial\, v_{0j,V}}{\partial\, z}\, \dot{z} \,+\, a^R_{0j,V} \\ \alpha_{0j,V} &= \left[\, 0_{3\times3} \;\; \mathrm{I}_{3\times3} \;\; \ldots d_{j,V} \ldots \right] \dot{z} \,+\, \omega_{0V,V} \times \omega_{0j,V} + \dot{d}_{j,V}\,\dot{y}_j \;=\; \frac{\partial\, \omega_{0j,V}}{\partial\, z}\, \dot{z} \,+\, \alpha^R_{0j,V} \end{aligned} \tag{9}$$

where the vector

$$z = \left[\, v_x \; v_y \; v_z \;\; \omega_x \; \omega_y \; \omega_z \;\; \dot{y}_1 \ldots \dot{y}_n \right]^T \tag{10}$$

collects the generalized velocities of the vehicle model. The symbols $\mathrm{I}_{3\times3}$ and $0_{3\times3}$ represent 3×3 matrices of identity and zeros. The $3\times f$ matrices $\partial\, v_{0j,V}/\partial\, z_j$ and $\partial\, \omega_{0j,V}/\partial\, z_j$, where f denotes the number of degrees of freedom, represent the partial velocities and partial angular velocities of the absolute body j motion. The symbols $a^R_{0j,V}$ and $\alpha^R_{0j,V}$ abbreviate the remaining acceleration and the remaining angular acceleration terms, which do not explicitly depend on the time derivatives of the generalized velocities.

Passenger car suspensions force the knuckles to perform rather complex nonlinear but smooth motions relative to the chassis or the vehicle-fixed reference frame V respectively. In addition, the damper elements in a vehicle suspension systems reduce the relative velocities $\dot{y}_j$ to moderate values. As a consequence, the terms $\dot{t}_{j,V}\,\dot{y}_j$ and $\dot{d}_{j,V}\,\dot{y}_j$ can be neglected compared to the other terms in the remaining acceleration and the remaining angular acceleration which results in a non-perfect multibody model, but safes a significant amount on computation effort and still provides an acceptable accuracy [17].

Chassis

The first body, the chassis, represents a special case, because the vehicle-fixed reference V frame is fixed to the chassis. As a consequence, the position vector $r_{V1,V} = r_{VC,V}$ is constant and the rotation matrix is simply defined by the 3×3 matrix of identity, $A_{V1} = A_{VC} = \mathrm{I}_{3\times3}$. Then

$$\frac{\partial\, v_{0C,V}}{\partial\, z} = \left[\, \mathrm{I}_{3\times3} \;\; \tilde{r}^T_{VC,V} \;\; 0_{3\times f_r} \right] \qquad \text{and} \qquad \frac{\partial\, \omega_{0C,V}}{\partial\, z} = \left[\, 0_{3\times3} \;\; \mathrm{I}_{3\times3} \;\; 0_{3\times f_r} \right] \tag{11}$$

provide the partial velocities and the partial angular velocities of the chassis, where $f_r = f - 6$ denotes the degrees of freedom of the motions relative to the chassis.

Generic Suspension

The kinematics of standard suspension systems, like the double wishbone, the MacPherson, or the multi-link suspension, can be solved online or approximated by lookup tables or more efficiently by smooth two-dimensional functions [18]. Regardless of the type of an independent suspension the position and orientation of the knuckle fixed reference frame K relative to the chassis or vehicle-fixed frame V can be described by a position vector and a rotation matrix

$$r_{VW,V} = r_{VW,D} + \begin{bmatrix} \xi \\ \eta \\ \zeta \end{bmatrix} \quad \text{and} \quad A_{VK} = A_\gamma\, A_\alpha\, A_\beta \tag{12}$$

where $r_{VW,D}$ describes the design position of the wheel center W, which on a balanced wheel is located on the wheel rotation axis and hence fixed to the knuckle. The rotation matrix is composed of three elementary rotations, where γ describes the steer motion, α the wheel camber, and β the pitch motion of the knuckle.

In particular at kinematic and compliance (KnC) tests, the wheel center W is used as a reference point to monitore and measure the knuckle/wheel movements. The coordinates $\xi = \xi(h,s)$, $\eta = \eta(h,s)$, $\zeta = \zeta(h,s)$ as well as the rotation angles $\alpha = \alpha(h,s)$, $\beta = \beta(h,s)$, $\gamma = \gamma(h,s)$ depend on the hub and steer motions h and s. In general, the hub motion can be described by the vertical displacement of the wheel center, $\zeta = h$. A least square approximation of measured or computed KnC tests delivers the design kinematic parameters, which for a typical double wishbone suspension on the left front wheel are listed in Table 1. It provides column by column the parameter sets required for the two-dimensional design kinematic functions $f = f(h,s)$, where h and s represent the hub and the steer motion. The columns hold for the constraint knuckle motions $\xi = \xi(h,s)$ to $\gamma = \gamma(h,s)$, the spring and damper displacements $u_S = u_S(h,s)$ and $u_D = u_D(h,s)$, as well as the vertical movement $z_{arb} = z_{arb}(h,s)$ of the anti-roll bar attachment point. Each parameter set consists of the range limits (`dh`, `ds`), the initial inclinations (`dfdh0`, `dfds0`), as well as the four center (`fp0`, `f0p`, `f0n`, `fn0`) and the four corner points (`fpp`, `fpn`, `fnp`, `fnn`) as defined in [18].

Table 1: Design kinematics parameters for a typical double wishbone front left suspension including force element displacements

ξ	η	α	β	γ	u_S	u_D	z_{arb}	
+0.08096	+0.08096	+0.08096	+0.08096	+0.08096	+0.08096	+0.08096	+0.08096	dh
+0.07240	+0.07240	+0.07240	+0.07240	+0.07240	+0.07240	+0.07240	+0.07240	ds
-0.02765	-0.07112	+0.44734	-0.32329	+0.11453	+0.89260	+0.89323	+0.67524	dfdh0
+0.30806	-0.14963	+1.20972	+1.20120	-8.21459	-0.19082	-0.16794	-0.01680	dfds0
+0.01559	-0.03140	+0.11704	+0.10749	-0.57684	+0.01238	+0.05418	+0.05251	fpp=f(+dh,+ds)
-0.00218	-0.01604	+0.05305	-0.02603	+0.00908	+0.07213	+0.07291	+0.05257	fp0=f(+dh, 0)
-0.03338	-0.01630	-0.12277	-0.11642	+0.78398	+0.01970	+0.07544	+0.05581	fpn=f(+dh,-ds)
+0.01826	-0.01635	+0.06099	+0.10629	-0.61014	-0.04529	-0.01864	-0.00030	f0p=f(0 ,+ds)
-0.03167	+0.00089	-0.14875	-0.05932	+0.79015	-0.04802	+0.00026	+0.00311	f0n=f(0 ,-ds)
+0.02081	-0.02134	+0.02840	+0.11802	-0.63890	-0.10653	-0.08846	-0.05699	fnp=f(-dh,+ds)
+0.00224	-0.00420	-0.02389	+0.02663	-0.00885	-0.07249	-0.07190	-0.05673	fn0=f(-dh, 0)
-0.02946	-0.00217	-0.14831	-0.02219	+0.78449	-0.11015	-0.07223	-0.05396	fnn=f(-dh,-ds)

The Matlab function provided in the following Listing computes the kinematics of a generic suspension modeled by the design kinematics. It provides the orientation of the knuckle-fixed reference frame, the momentary position of the wheel center which serves as a reference point for the knuckle motion, as well as the corresponding partial velocity and partial angular velocity. The 3×1-vector `ufe` collects the displacements of the spring u_S, the damper u_D, and the vertical movement z_{arb} of the anti-roll bar. The 3×2-matrix `dufedyf` contains the changes of `ufe` with respect to the hub and steer motions collected in the 2×1-vector `yk = [h;s]`. They are used within the VTC environment to compute the contribution of the suspension forces to the vector of generalized forces directly via the virtual power. The additional 5×1 output vector `ao` collects the constraint motions resulting from the Matlab function `dk_fun`, which evaluates the two-dimensional functions as described in [18].

Listing: Matlab function computing the kinematics of a generic suspension via the design kinematics

```
function ...    % v t c   u t i l i t y
[ avk ...       % orientation of knuckle fixed frame
, dkv ...       % part. angular velocities knuckle
, rvwv ...      % position of wheel center
, twv ...       % partial velocities wheel center
, ufe ...       % force element displacements
, dufedyf ...   % change of ufe due to yf
, ao ...        % additional output
] = dk_susp ... % generic suspension via design kinematics
( yk ...        % generalized suspension coordinates yk = [ h; s ]
, rvkd ...      % design position of wheel center
, dkin ...      % matrix of design kinematics parameter
)

% constraint wheel motions ( yk(1) = hub, yk(2) = steer )
[ xw,dxwdyf(1),dxwdyf(2) ] = dk_fun( yk(1), yk(2), dkin(:,1) );
[ yw,dywdyf(1),dywdyf(2) ] = dk_fun( yk(1), yk(2), dkin(:,2) );
[ al,daldyf(1),daldyf(2) ] = dk_fun( yk(1), yk(2), dkin(:,3) );
[ be,dbedyf(1),dbedyf(2) ] = dk_fun( yk(1), yk(2), dkin(:,4) );
[ ga,dgadyf(1),dgadyf(2) ] = dk_fun( yk(1), yk(2), dkin(:,5) );

% sine- and cosine functions as well as combinations
sal = sin(al);  sbe = sin(be);  sga = sin(ga);
cal = cos(al);  cbe = cos(be);  cga = cos(ga);
salsbe = sal*sbe; salcbe = sal*cbe; calsga = cal*sga; calcga = cal*cga;

% rotation matrix of chassis -> knuckle (elementary rotations: ga-al-be)
avk(1,1) =  cbe*cga - salsbe*sga;
avk(2,1) =  cbe*sga + salsbe*cga;
avk(3,1) = -sbe*cal;
avk(1,2) = -calsga;
avk(2,2) =  calcga;
avk(3,2) =  sal;
avk(1,3) =  sbe*cga + salcbe*sga;
avk(2,3) =  sbe*sga - salcbe*cga;
avk(3,3) =  cal*cbe;

% partial angular velocities due to hub and steer
dkv = zeros(3,2);
for j=1:2
  dkv(1,j) = cga*daldyf(j) - calsga*dbedyf(j);
  dkv(2,j) = sga*daldyf(j) + calcga*dbedyf(j);
  dkv(3,j) =                    sal*dbedyf(j)  +  dgadyf(j);
end

% actual position of wheel center
rvwv = [ rvkd(1)+xw; rvkd(2)+yw; rvkd(3)+yk(1) ];

% partial velocities  due to hub and steer
```

```
twv = [ dxwdyf(1)  dxwdyf(2) ; ...
        dywdyf(1)  dywdyf(2) ; ...
            1          0     ];

% displacements and partial derivatives of force elements
[ ufe(1),dufedyf(1,1),dufedyf(1,2) ] = dk_fun( yk(1), yk(2), dkin(:,6) );
[ ufe(2),dufedyf(2,1),dufedyf(2,2) ] = dk_fun( yk(1), yk(2), dkin(:,7) );
[ ufe(3),dufedyf(3,1),dufedyf(3,2) ] = dk_fun( yk(1), yk(2), dkin(:,8) );

% provide constraint motions as additional output
ao  =  [ xw; yw;  al; be; ga ];

end
```

The generic suspension model provides the position of the wheel center rvwv $\rightarrow r_{VW,V}$ and the orientation of the knuckle avk $\rightarrow A_{VK}$ relative to the vehicle-fixed reference frame V as well as the 3×2-matrices dkv $\rightarrow d_{K,V}$ and twv $\rightarrow t_{W,V}$ which provide the partial angular velocities of the knuckle and the partial velocity of the wheel center. The velocity of the wheel center and the angular velocity of the wheel are then determined by

$$v_{0W,V} = v_{0V,V} + \omega_{0V,V} \times r_{VW,V} + t_{W,V} \begin{bmatrix} \dot{h} \\ \dot{s} \end{bmatrix} \quad \text{and} \quad \omega_{0W,V} = \omega_{0V,V} + d_{K,V} \begin{bmatrix} \dot{h} \\ \dot{s} \end{bmatrix} + e_{yW,V}\, \dot{\varphi} \tag{13}$$

where $e_{yW,V} = A_{VK}\, e_{yW,D}$ provides the knuckle-fixed wheel rotation axis and $\omega_{KW,V} = e_{yW,V}\, \dot{\varphi}$ describes the angular velocity of the wheel rotation relativ to the knuckle. The momentary position of the knuckle center K and its partial velocities are defined by

$$r_{VK,V} = r_{VW,V} + A_{VK}\, r_{WK,D} = r_{VW,V} + r_{WK,V} \quad \text{and} \quad t_{K,V} = t_{W,V} + d_{K,V} \times r_{WK,V} \tag{14}$$

where $r_{WK,D}$ denotes the design position of the knuckle center K relative to the wheel center W.

Equations of Motion

The state of a generic VTC model, as proposed here, is defined by $f = 18$ generalized coordinates and $f = 18$ generalized velocities collected in the vectors

$$\begin{aligned} y &= \left[\, x_V \;\, y_V \;\, z_V \;\, \phi_V \;\, \theta_V \;\, \psi_V \quad h_1 \;\, s_1 \quad h_2 \;\, u_2 \quad h_3 \;\, u_3 \quad h_4 \;\, u_4 \quad \varphi_1 \;\, \varphi_2 \;\, \varphi_3 \;\, \varphi_4 \,\right]^T \\ z &= \left[\, v_x \;\, v_y \;\, v_z \;\, \omega_x \;\, \omega_y \;\, \omega_z \quad \dot{h}_1 \;\, \dot{s}_1 \quad \dot{h}_2 \;\, \dot{u}_2 \quad \dot{h}_3 \;\, \dot{u}_3 \quad \dot{h}_4 \;\, \dot{u}_4 \quad \dot{\varphi}_1 \;\, \dot{\varphi}_2 \;\, \dot{\varphi}_3 \;\, \dot{\varphi}_4 \,\right]^T \end{aligned} \tag{15}$$

Jourdain's principle of virtual power delivers the equations of motion as a set of two first order nonlinear systems of differential equations

$$\dot{y} = K(y)\, z \quad \text{and} \quad M(y)\, \dot{z} = q(y,\, z,\, u,\, w) \tag{16}$$

where the vectors u and w collect all model inputs and additional dynamic states, required for dynamic tire and dynamic suspension forces. A kinematic matrix K which does not coincide with the matrix of identity, makes it possible to define non-trivial generalized velocities, as done here in (2) for the overall vehicle motions. The elements of the mass matrix M and the vector of generalized forces and torques q applied to the vehicle are generated for the $n = 9$ bodies of the VTC model via

$$M = \sum_{j=1}^{n} \left\{ \left(\frac{\partial v_{0j,V}}{\partial z} \right)^T m_j\, \frac{\partial v_{0j,V}}{\partial z} + \left(\frac{\partial \omega_{0j,V}}{\partial z} \right)^T \Theta_{j,V}\, \frac{\partial \omega_{0j,V}}{\partial z} \right\} \tag{17}$$

$$q = \sum_{j=1}^{n} \left\{ \left(\frac{\partial v_{0j,V}}{\partial z} \right)^T \left[F^a_{j,V} - m_j\, a^R_{0j,V} \right] + \left(\frac{\partial \omega_{0j,V}}{\partial z} \right)^T \left[T^a_{j,V} - \Theta_{j,V} \alpha^R_{0j,V} - \omega_{0j,V} \times \Theta_{j,V} \omega_{0j,V} \right] \right\} \tag{18}$$

where m_j and $\Theta_{j,V}$ describe the mass and inertia of body j, $F^a_{j,V}$ and $T^a_{j,V}$ represent the resulting vectors of the forces and torques applied to body j. Equations (6) and (9) provide the angular velocities $\omega_{0j,V}$, the partial velocities $\partial v_{0j,V} \partial z$, the partial angular velocities $\partial \omega_{0j,V}/\partial z$, as well as the remaining acceleration $a^R_{0j,V}$ and the remaining angular acceleration $\alpha^R_{0j,V}$. The partial velocities of the front right knuckle (K2) and the front right wheel (W2) are, for example, defined by

$$\begin{aligned} \frac{\partial\, v_{0K2,V}}{\partial\, z} &= \left[\, \mathrm{I}_{3\times3} \quad \tilde{r}^T_{VK2,V} \quad 0_{3\times2} \quad t_{K2,V} \quad 0_{3\times2} \quad 0_{3\times2} \quad 0_{3\times1} \quad 0_{3\times1} \quad 0_{3\times1} \quad 0_{3\times1} \,\right] \\ \frac{\partial\, \omega_{0K2,V}}{\partial\, z} &= \left[\, 0_{3\times3} \quad \mathrm{I}_{3\times3} \quad 0_{3\times2} \quad d_{K2,V} \quad 0_{3\times2} \quad 0_{3\times2} \quad 0_{3\times1} \quad 0_{3\times1} \quad 0_{3\times1} \quad 0_{3\times1} \,\right] \end{aligned} \tag{19}$$

$$\begin{aligned} \frac{\partial\, v_{0W2,V}}{\partial\, z} &= \left[\, \mathrm{I}_{3\times3} \quad \tilde{r}^T_{VW2,V} \quad 0_{3\times2} \quad t_{W2,V} \quad 0_{3\times2} \quad 0_{3\times2} \quad 0_{3\times1} \quad 0_{3\times1} \quad 0_{3\times1} \quad 0_{3\times1} \,\right] \\ \frac{\partial\, \omega_{0W2,V}}{\partial\, z} &= \left[\, 0_{3\times3} \quad \mathrm{I}_{3\times3} \quad 0_{3\times2} \quad d_{W2,V} \quad 0_{3\times2} \quad 0_{3\times2} \quad 0_{3\times1} \quad e_{yW2,V} \quad 0_{3\times1} \quad 0_{3\times1} \,\right] \end{aligned} \tag{20}$$

The TMeasy model [9] provides the tire forces $F_{T1,0}$ to $F_{T4,0}$ and the torques $T_{T1,0}$ to $T_{T4,0}$ applied to the four wheel centers. In particular, the slip based longitudinal and lateral tire forces strongly depend on the velocity state v_{0W} and ω_{0W} of the wheel. The velocity state of the wheel depends, according to (13), on the velocity state of the vehicle ($v_{0V,V}$ and $\omega_{0V,V}$) and on the kinematical properties of the suspension systems represented by the symbols $t_{W,V}$, $d_{K,V}$, and $e_{yW,V}$, which describe the partial velocity of the wheel center, the partial angular velocity of the knuckle, and the position of the wheel rotation axis. Hence, neglecting the suspension kinematics partly or completely, as done in simplified vehicle models, inevitably results in poorly modeled tire forces and tire torques.

The vehicle dynamics represented by (16) is driven by the vector of generalized forces and torques. The contribution of front right tire, part of the front right knuckle (K2) and wheel (W2) combination, to the vector of generalized forces and torques is, for example, provided by

$$\begin{aligned} \text{overall vehicle:} \quad & q_{1:6} = q_{1:6} + \begin{bmatrix} F_{T2,V} \\ T_{T2,V} + r_{VW2,V} \times F_{T2,V}^T \end{bmatrix} \\ \text{hub and steer motions front right:} \quad & q_{9:10} = q_{9:10} + t_{W2,V}^T \, F_{T2,V} + d_{K2,V}^T \, T_{T2,V} \\ \text{wheel rotation front right:} \quad & q_{16} = q_{16} + e_{yW,V}^T \, T_{T2,V} \end{aligned} \tag{21}$$

The relations $F_{T2,V} = A_{0V}^T \, F_{T2,0}$ and $T_{T2,V} = A_{0V}^T \, T_{T2,0}$ transform the resulting tire force vector and the resulting tire torque vector from the earth-fixed into the vehicle-fixed frame. The amount of contribution depends on the partial velocity of the wheel center $t_{W2,V}$, the partial angular velocity of the knuckle $d_{K2,V}$, and the wheel rotation axis $e_{yW,V}$. Tire forces, which support and guide the vehicle, may change very quickly and can increase to considerable values, in particular in critical driving situations. That is why, even rather small changes in the kinematical suspension properties, represented by the symbols $t_{W,V}$, $d_{K,V}$, and $e_{yW,V}$, result in significant contributions to the vector of generalized force and torques. Which magnifies the error in neglecting the specific properties of the suspension kinematics.

Example: Braking in a Turn

The numerical solution of differential equations, like the ones in (16), is discussed in [19]. A straightforward implementation of the virtual test car (VTC) entirely realized in MATLAB provides an easy to use simulation environment including plotting and animation facilities, Figure 2. As typical for standard passenger cars on dry road, the left plot in Figure 2

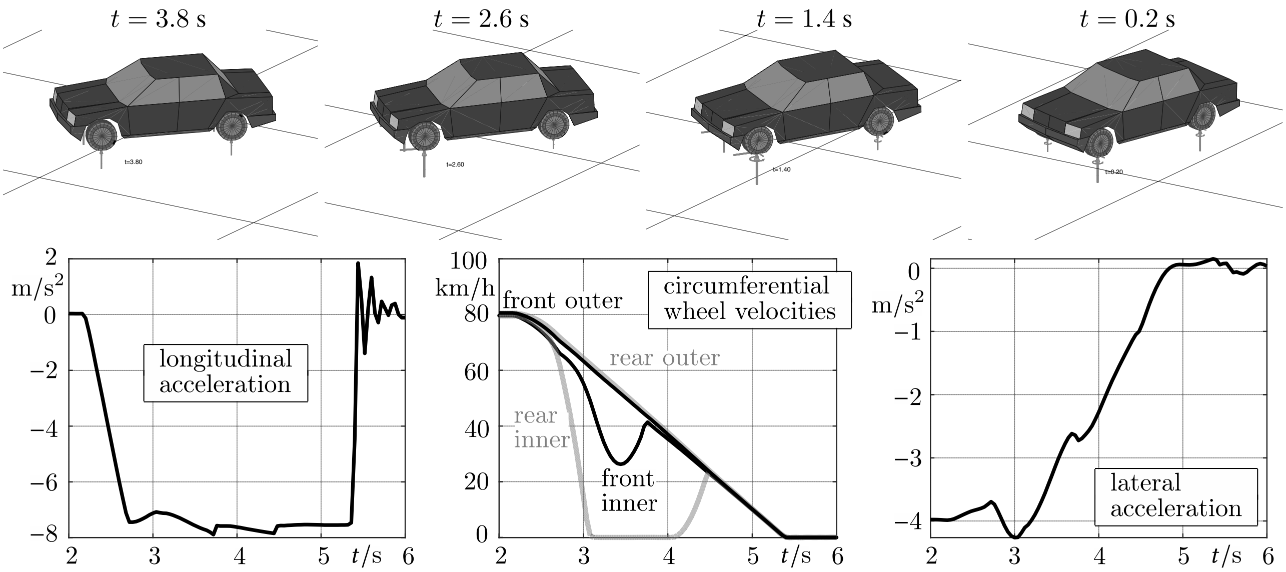

Figure 2: Emergency braking in a turn without ABS of a typical midsize passenger car illustrated by animation screenshots and plots.

indicates a maximum deceleration of approximately 8 m/s^2. The wheel load transfer from inner to outer during cornering and from rear to front when braking causes the inner rear wheel to lock in the time interval $t \approx 3$ s to $t \approx 4$ s, center plot in Figure 2. The VTC model handles wheel lock without any problems and the TMeasy tire model provides a smooth transition to stand still in addition.

The numerical integration in the time interval $2 \leq t \leq 6$ s performed with the standard MATLAB solver ode45, an explicit Runge-Kutta formula of order 4 and 5 with step size control, took a 2,7 GHz Quad-Core Intel Core i7 just 4.72 seconds. This is already close to real-time performance $(6-2)/4.72 = 0.85$ even in the comparatively slow MATLAB interpretation mode.

Influence of the Suspension Kinematics on the Vehicle Dynamics

From a Standard to a Simplified Suspension Kinematics

Table 1 provides the design kinematics parameter matrix for the front left suspension of a typical passenger car. The initial inclinations $d\alpha/dh$ = `+0.44734` rad(m, $d\beta/dh$ = `-0.32329` rad(m, and $d\beta/dh$ = `+0.11453` rad(m indicate that the knuckle performs significant rotations induced by the hub motion. As typical for front axle suspensions, the first, second, and third rotation produces a partial camber compensation, counteracts the brake pitch, and generates a slight self-steering effect. The axis of the knuckle-fixed coordinate system are parallel to the corresponding axis of the vehicle-fixed reference frame. That is why, the design kinematics takes `f00=f(0,0)=0` for granted. Then, center points with different absolute values at vanishing steering angles (`s=0`), like `fp0`$_\alpha$ $= \alpha(+dh, 0)$ = `+0.05305` rad and `fn0`$_\alpha$ $= \alpha(-dh, 0)$ = `-0.02389` rad specify a nonlinear behavior, which in general is not a simple side effect but a well design feature of the suspension kinematics. The design kinematics approach makes it easy to tune or design the suspension kinematics. Replacing the first row in the parameter matrix of Table 1 by

```
+0.00000   +0.00000   +0.00000   +0.00000   +0.00000   +0.08096   +0.08096   +0.08096   dh
```

just switches off the influence of the hub motion h on the constraint motions ξ, η, α, β, and γ by leaving the force element displacements u_S, u_D, and z_{arb} unchanged. Simple 4-wheel vehicle models just take the steer motions into consideration by neglecting the vertical suspension motions in addition, thus providing a far worse approximation.

Transient Vehicle Response

The DIN ISO directive 7401 lists the step steer input as one of the standard open loop maneuvers to reveal insight into the transient response of vehicles. In practice, an ideal step input is not possible. The VTC environment realizes the steer input s at the front and optionally at the rear axle via the rack displacements. Table 2 provides the time history of the

Table 2: Define step steer input within the VTC environment via lookup tables

0.0000	0.5000	0.6000	6.0000	time sample points τ_{Si} in s
0.0000	0.0000	-0.0050	-0.0050	steer input front left $\varrho_1(t_{Si})$ in m
0.0000	0.0000	-0.0050	-0.0050	steer input front right $\varrho_2(t_{Si})$ in m

steer inputs at the front axle which correspond here to the rack displacement $\varrho_1 = \varrho_2 = \varrho$ of a standard rack and pinion steering system. The rear wheels are not steered in this example $\varrho_3 = \varrho_4 = 0$. The steering forces applied to the knuckles 1 to 4 are defined by

$$F_{Si} = c_{Si}\left(\varrho_i - s_i\right) + d_{Si}\left(\dot{\varrho}_i - \dot{s}_i\right), \quad i = 1(1)4 \tag{22}$$

The constants c_{Si}, d_{Si} summarize the stiffness and damping properties of the tie rods and the steering lever. The time histories of the steer inputs deliver also their time derivatives $\dot{\varrho}_1$ to $\dot{\varrho}_4$. The steer motions of the knuckles s_1 to s_4 and their derivatives $\dot{s}_1$ to $\dot{s}_4$ are part of the vectors of generalized coordinates y and generalized velocities z as defined in (15). Table 2 approximates the step by a continuous ramp, where the rack is moved in the time interval $0.5 \le \tau_S \le 0.6$ s from its center position $s_1 = s_2 = 0$ to the right $s_1 = s_2 = -5$ mm and then ($\tau_S > 0.6$ s) kept constant. This input generates the wheel steering angles displayed as dotted black and dotted grey lines in plot (a) of Figure 3.

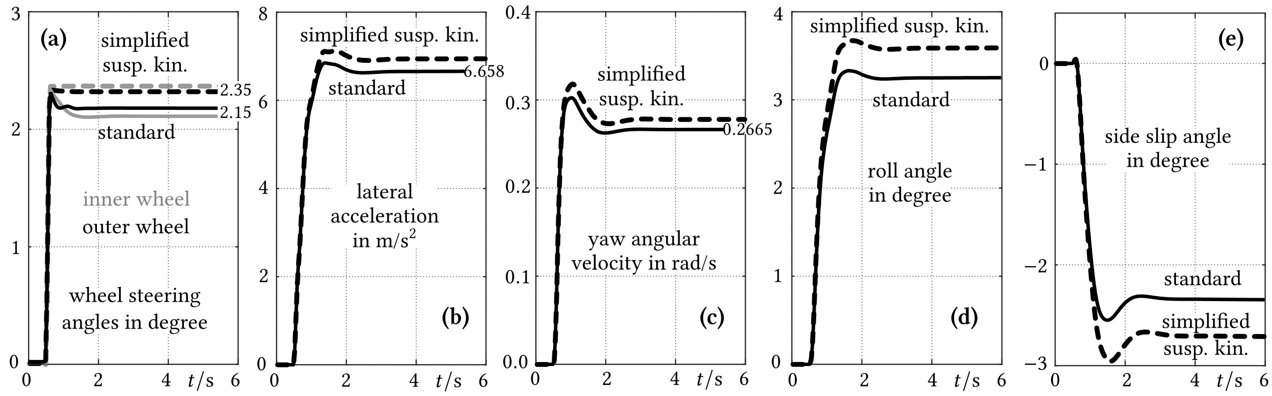

Figure 3: VTC step steer results, where solid and broken lines characterize vehicles with standard and simplified suspension kinematics

The VTC model represents here a fullsize passenger car with a wheel base of $a = 2.9$ m, a track width of $s \approx 1.5$ m, and wheel loads of $F_{z1} = F_{z2} = 5.39$ kN and $F_{z3} = F_{z4} = 5.06$ kN at the front and rear. The steady state values of the lateral acceleration $a_y = v^2/R = 6.658$ m/s^2 and the yaw angular velocity $\dot{\psi} = v/R = 0.2665$ rad/s deliver a cornering radius of $R = 94$ m and a vehicle velocity of $v = 25$ m/s in this example. A PI-controller keeps the vehicle velocity constant during the whole manuever by generating appropriate drive torques applied to the rear wheels.

The plots in Figure 3 compare the results of the VTC model with standard double wishbone suspensions at the front and the rear to a VTC model where the influence of the hub motion on the constraint suspension motions is completely switched off. As a consequence, the wheel steering angles of the simplified VTC model, represented by the dotted gray and dotted black lines in plot (a) of Figure 3, correspond perfectly to the step or more precisely to the ramp steer input. The nonlinear suspension kinematics of the front wheels incorporates a roll steering which reduces the steering angles with increasing body roll. That is why the steering angles drop down in the average from 2.35 to 2.15 degree when the roll angle, solid line in plot (c) of Figure 3, increases from 0 to 3.25 degree. This roll steer effect is a well designed feature of the suspension kinematics. It automatically reduces the impact of the steer input at fast cornering but keeps the maneuverability in the lower lateral acceleration range.

For a fair comparison of the standard vehicle to a vehicle with simplified kinematics the steer input of the standard vehicle is increased such that both VTC models end up in the same lateral acceleration. The results are displayed in Figure 4, where the steering wheel angles, plotted on the left, are zoomed to the interesting range from 2.0 to 2.5 degrees. In general, the kinematics of passenger car steering linkages is designed according to the Ackermann geometry which results in larger steering angles at the curve inner wheel compared to the curve outer wheel. The roll steering effect of the VTC model with the standard suspension kinematics even counteracts the Ackermann geometry, solid black and grey lines in the left plot of Figure 4. This is a smart suspension design, because during fast cornering the outer wheels are much more loaded than the inner ones and hence the steering angle of the outer wheel is the one that counts.

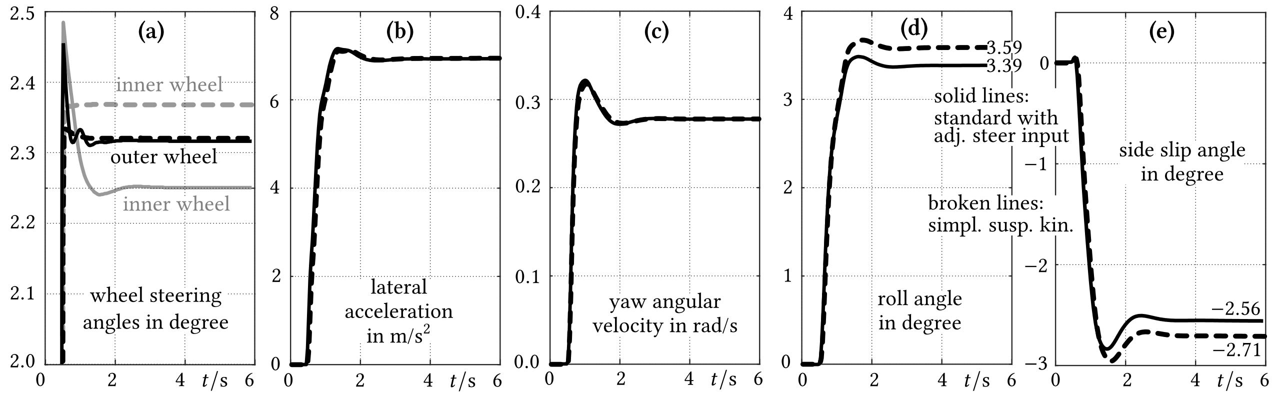

Figure 4: VTC step steer results with simplified and standard suspension kinematics with adjusted steer input

Both VTC models end up now in the same lateral acceleration and the same yaw angular velocity, plots (b) and (c) in Figure 4. But, the time histories of the roll angle and the side slip angle still differ in their steady state values, plots (d) and (e) in Figure 4.

Standard Versus Simplified Kinematics

In practice, the suspension kinematics of a passenger car is carefully designed to meet certain requests arising from the longitudinal and lateral dynamics [20]. The Figures 5 and 6 show the three-dimensional motions of the front left knuckle for the VTC model with the simplified suspension kinematics and for the VTC model with the standard suspension kinematics.

At real passenger car suspension systems a steer motion causes the knuckle to rotate about the inclined kingpin axis which in addition has a longitudinal and lateral offset to the wheel center. That is why, the centers 1 and 2 of the steered front wheels perform longitudinal ξ and lateral η motions as well as elementary rotations α, β, γ about the x-, y-, and z-axis which in case of the simplified suspension entirely depend on the steer input s, Figure 5. The vertical displacements of the wheel centers are unconstrained and described by the hub motion $\zeta = h$. Bump stops in the suspension systems restrict the jounce motions ($h > 0$) at the curve outer wheels 2 and 4, upper right plot in Figures 5 and 6. The plots in Figure 6 reveal the complexity of standard passenger car suspension systems. The distinct longitudinal motions ξ of the wheel center 3 and the distinct pitch rotations β of the knuckle 3 indicate for example the ability of the rear suspension to reduce a brake pitch. The lateral motions η and the rotations α about the x-axis provide the roll support and a partial camber compensation. The former brings down the roll angle from 3.59 to 3.39 degrees, plot (d) of Figure 4. The roll support and the camber compensation at the front and rear wheels, which are carefully coordinated to each other, reduce further on the side slip angle from -2.71 to -2.56 degrees, plot (e) of Figure 4.

The steering forces $F_S = [F_{S1}\ F_{S2}\ F_{S3}\ F_{S4}]^T$ and the driving torques $T_D = [T_{D1}\ T_{D2}\ T_{D3}\ T_{D4}]^T$ as well as the braking torques $T_B = [T_{B1}\ T_{B2}\ T_{B3}\ T_{B4}]^T$ define the inputs of the VTC model. The steering forces are directly applied to the knuckles. Each of the driving torques acts between the chassis and the corresponding wheel at conventional drive trains or between knuckle and wheel in case of wheel motors. The braking torques specify the maximum torques usually defined by the braking pressures distributed to the wheels. An enhanced dry friction model, as described in [20], generates the individual braking torque acting between knuckle and wheel. All inputs may be defined as simple feed forward time

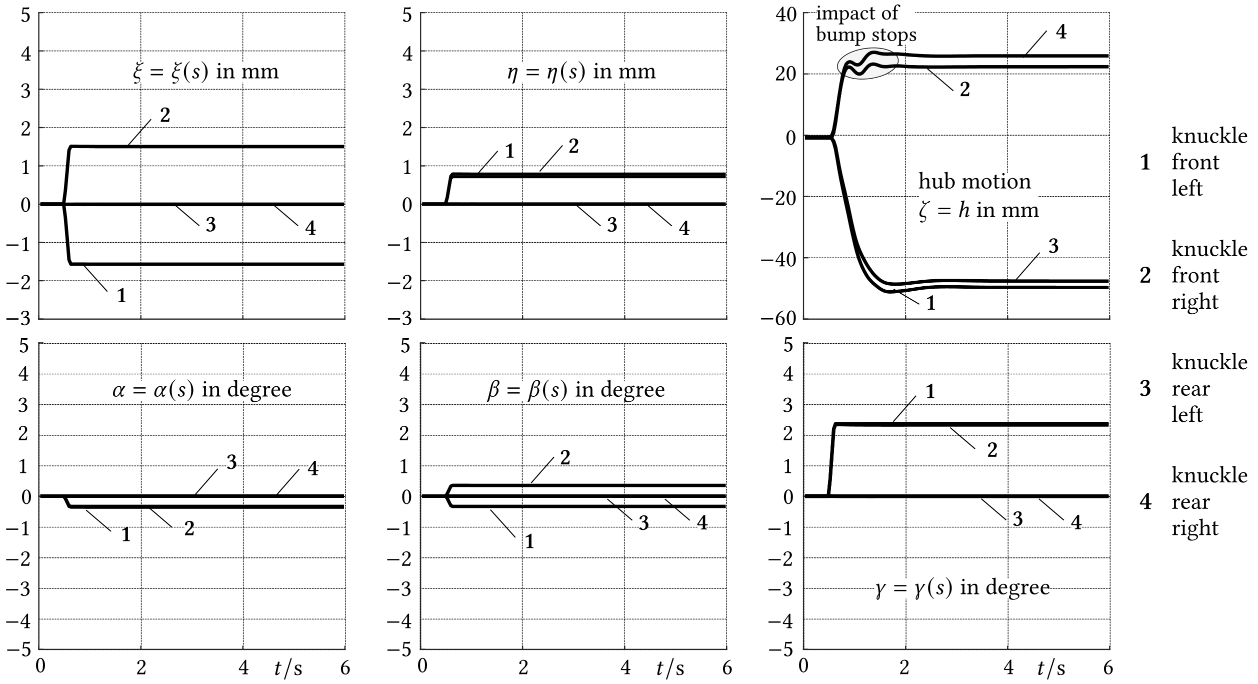

Figure 5: Simplified suspension kinematics neglecting hub influence

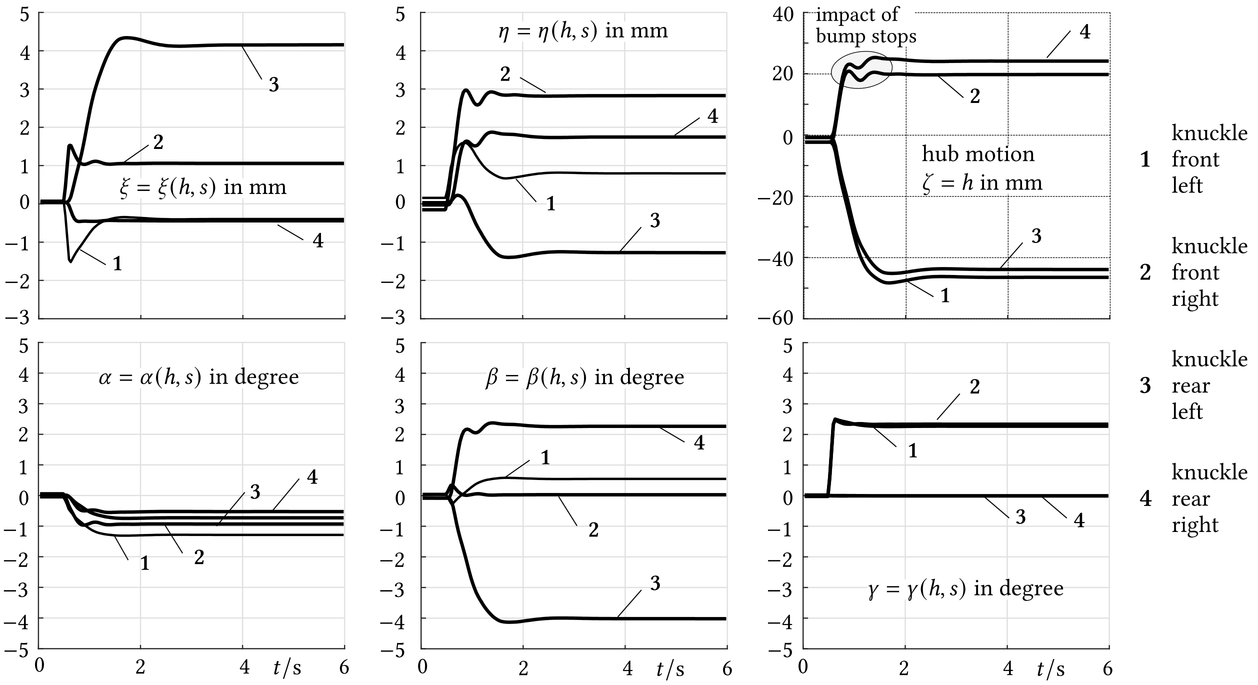

Figure 6: Standard suspension kinematics with adjusted step steer input

histories or provided by external controllers or by the output of additional subsystems. Hence, the VTC environment is able to simulate vehicles with all kind of steering, driving and braking modes.

Jourdain's principle combined with non-trivial generalized velocities and the idea of a non-perfect multibody system approach result in equations of motion of minimal complexity. A partial implicit solver, as described in [21], provides an extremely fast numerical solution of sufficient accuracy and stability.

Consequences

Human drivers and automated drivers too are very sensitive to the roll angle and to the side slip angle, in particular. Hence, a vehicle model which neglects some or all properties of the suspension kinematics is not able to reproduce the dynamics of a real passenger car with reliable accuracy. Virtual tests to investigate the dynamics and the stability of vehicles as well as the development and further improvement of driver assistance systems require at least vehicle models which incorporate the nonlinearities of the suspension kinematics. Otherwise just basic studies will be possible, which of course may serve as starting points for further and reliable investigations.

Conclusion

Simplified vehicle models, like the classical bicycle model, 4-wheel vehicle models, or even three-dimensional vehicle models neglecting the specific kinematical properties of the suspension systems, are not able to reproduce the dynamics of vehicles properly. Such models are restricted to basic studies. The VTC environment takes the three-dimensional motions of the chassis, four knuckles, and four wheels into account. The generic design kinematics suspension model is able to describe the nonlinear properties of standard passenger car suspension systems with sufficient accuracy and with a minimum of computation effort. The VTC model operated with the TMeasy tire model is valid in any driving situation. A straightforward implementation of the virtual test car (VTC) entirely realized in MATLAB provides an easy to use simulation environment including plotting and animation facilities. A VTC implementation coded in C achieves on a standard personal computer with a 2,7 GHz Quad-Core Intel Core i7 a real-time factor (real-time/cpu-time) of 160 which is magnitudes faster than real-time. Thus making the Virtual Test Car to an ideal platform for modern simulation tasks.

References

[1] . Bruni S. et al. (2020) State-of-the-art and challenges of railway and road vehicle dynamics with multibody dynamics approaches. *Multibody System Dynamics 49, 1-32*.

[2] Adams/Car. https://www.mscsoftware.com/de/product/adams-car, last accessed on March 11, 2022.

[3] RecurDyn. https://www.functionbay.org, last accessed on March 11, 2022.

[4] SIMPACK. https://www.3ds.com/products-services/simulia/products/simpack/, last accessed on March 11, 2022.

[5] CarSim. https://www.carsim.com, last accessed on March 11, 2022.

[6] CarMaker. https://ipg-automotive.com/en/products-solutions/software/carmaker/, last accessed on March 11, 2022.

[7] . DYNA4. https://www.vector.com/int/en/products/products-a-z/software/dyna4/, last accessed on March 11, 2022.

[8] Pacejka, H. B. (2002) Tire and Vehicle Dynamics, Butterworth-Heinemann, Oxford.

[9] Rill, G. (2013) TMeasy – The Handling Tire Model for all Driving Situations. *Proceedings of the XV International Symposium on Dynamic Problems of Mechanics (DINAME)*

[10] Rill, G. (2006) Vehicle Modeling by Subsystems. *Journal of the Brazilian Society of Mechanical Sciences & Engineering - ABCM 4, 431-443*.

[11] Rill, G. (1997) Vehicle Modeling for Real Time Applications. *Journal of the Brazilian Society of Mechanical Sciences - RBCM XIX.2 , pp. 192-206*.

[12] Gabiccini, M. et al. (2021) Analysis of driving styles of a GP2 car via minimum lap-time direct trajectory optimization *Multibody System Dynamics 53 pp. 85-113*. https://doi.org/10.1007/s11044-021-09789-7 last accessed on March 11, 2022.

[13] Vu, T. M. et al. (2021) Model Predictive Control for Autonomous Driving Vehicles. Electronics 2021, 10, 2593. https://doi.org/10.3390/electronics10212593.

[14] Rill, G. et al. (2019) VTT – a virtual test truck for modern simulation tasks. *Vehicle System Dynamics 0, 1-22*.

[15] Rill, G. (2019) Sophisticated but quite simple contact calculation for handling tire models. *Multibody System Dynamics 2, 131-153*.

[16] Rill, G. (1994) Simulation von Kraftfahrzeugen. Vieweg, Braunschweig/Wiesbaden. Reprint at https://www.researchgate.net/publication/317037037_Simulation_von_Kraftfahrzeugen#fullTextFileContent

[17] Rill, G. and Schaeffer, Th. (2017) Vehicle Modeling by non-perfect Multibody-Systems. *88th GAMM Annual Meeting, Weimar*. https://www.researchgate.net/publication/328049816_Vehicle_Modeling_by_non-perfect_Multibody_Systems#fullTextFileContent last accessed on March 11, 2022.

[18] Rill, G., Castro, A. A. (2020) A Novel Approach for Parametrization of Suspension Kinematics. *Advances in Dynamics of Vehicles on Roads and Tracks, 1848-1857*.

[19] Arnold, M. et al. (2011) Numerical methods in vehicle system dynamics: State of the art and current developments. *Vehicle System Dynamics 49, 1159-1207*.

[20] Rill, G. and Castro, A. A. (2020) Road Vehicle Dynamics: Fundamentals and Modeling with MATLAB® *CRC Press, Ed. 2*.

[21] Rill, G. (2006) A modified implicit Euler Algorithm for solving Vehicle Dynamic Equations. *Multibody System Dynamics, 15(1) 1-24*.